2130 BULLETIN OF THE CHEMICAL SOCIETY OF JAPAN, VOL. 52 (7), 2130—2135 (1979) [Vol. 52, No. 7

Phase Relations in the Sulfur-rich Portion of the Fe–V–S System at Temperatures between 520 and 814 °C

Hiroaki Wada
National Institute for Researches in Inorganic Materials, Namiki 1-1,
Sakura-mura, Niihari-gun, Ibaraki 300-31

(Received January 25, 1979)

An equilibrium study of a part of the Fe–V–S system at sections with atomic Fe:V ratios 1:1, 3:2, and 71:29 was carried out. A gravimetric method using a quartz spring balance was employed in the range of $\log(P_{S_2}/\text{atm}) = -4$ to -0.8 at temperatures between 520 and 814 °C. Phase relations in the sulfur-rich portion of the Fe–V–S system were examined on the basis of the P_{S_2}-T-X relation and X-ray analyses of the quenched specimens. The phase diagram of the Fe–V–S system was tentatively constructed at about 570 °C. The compositional dependence of the lattice parameters of the $(Fe,V)_3S_4$ solid solution was studied from the crystallographic viewpoint.

The results of an equilibrium study of a part of the Fe–V–S system at sections with atomic Fe : V ratios 1 : 19, 13 : 37, and 7 : 13 were presented in an earlier publication.[1)] It has been reported that the Fe–V–S system has extensive solid solution phases, such as $(Fe,V)_5S_8$, $(Fe,V)_2S_3$, and $(Fe,V)_3S_4$, which have a lattice intermediate between the NiAs-type and the $Cd(OH)_2$ lattice. However, the solid solution fields of these phases have not yet been determined completely. The detailed phase relations in the Fe-rich portion of the composition triangle of FeS–VS–S are still obscure, in spite of the extensive studies of the binary systems FeS[2)] and VS.[3)]

The present study is a continuation of this work using a further series of samples in the Fe–V–S system. The author reports in this paper the results of the equilibrium study of a part of the Fe–V–S system at sections with atomic Fe : V ratios 1 : 1, 3 : 2, and 71 : 29. The main thermochemical study was carried out with a gravimetric method, which used a quartz spring balance at high temperatures, above 500°C. The P_{S_2} (equilibrium sulfur pressure)-T (temperature)-X(composition) relations and the compositional dependence of lattice constants of several phases were investigated.

Experimental

The sulfide samples with atomic Fe:V ratios 1:1, 3:2, and 71:29 were synthesized by heating the mechanical mixtures of reagent grade $VOSO_4 \cdot 3H_2O$ and $FeSO_4 \cdot (NH_4)_2SO_4 \cdot 6H_2O$ in an H_2S atmosphere at 1050 °C for 4 h and were then used as starting materials. The equilibrium study of these samples was carried out by thermogravimetry at temperatures between 520 and 814 °C. The partial pressure of sulfur was controlled within the range of the $\log(P_{S_2}/\text{atm})$, from -0.8 to -4, in an N_2–sulfur vapor system. The general experimental procedures, the apparatus, chemical analyses, and phase identification of quenched specimens are the same as those described in the previous paper.[1)]

A supplemental method employed in this study was the rigid silica tube, quench-type, annealing experiment. In experiments of this type the elements or previously synthesized sulfides were used as source materials. The bulk composition of the charge was adjusted correctly to the desired proportion by weighing on an analytical balance. All weighings were made to a precision of ±0.05 mg. The empty tube was weighed first, then with metal or sulfides inserted, and finally with sulfur added to them. Tubes thus prepared were heated in horizontal furnaces for various periods of time and at fixed temperatures, controlled to within ±3 °C. At the termination of a run the charge was quenched into cold water.

Results and Discussion

Composition versus P_{S_2} *Diagram in a Part of the Fe–V–S System.* The results of equilibrium studies of the Fe–V–S system at sections with atomic Fe:V ratios 1 : 1, 3 : 2, and 71 : 29 are shown graphically in Figs. 1—2 and 4. The variation of equilibrium sulfur pressure P_{S_2} with the composition of sulfides ($X = S/(Fe+V)$) are given as the isothermal curves, which were drawn by a smooth fitting of data points. The phases as revealed by X-ray diffraction of the quenched specimens are also shown in the figures. Some representative results of quench-type experiments are given in Table 1. In the following text of this paper, solid solution, liquid, and vapor are abbreviated as s.s., L, and v for convenience.

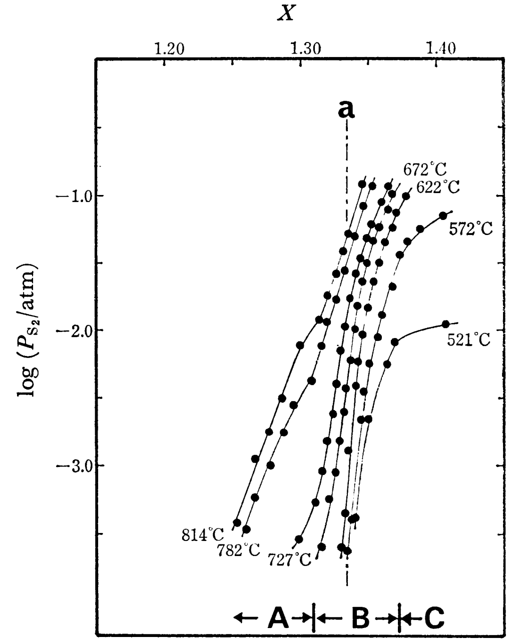

Fig. 1. P_{S_2}-composition ($X = S/(Fe+V)$) isotherms of $Fe_{0.50}V_{0.50}S_X$. Phase identifications of quenched specimens by X-ray powder diffraction method are shown in lower part of figure as follows A: $(Fe,V)_{1-\delta}S$ s.s. + $(Fe,V)_3S_4$ s.s. B: $(Fe_{0.50}V_{0.50})_3S_4$ s.s. C: $(Fe,V)_3S_4$ s.s. + FeS_2. The stoichiometric Fe+V: S = 3:4 composition is designated as the symbol a.

Table 1. Results of X-ray identification of the quenched specimens

Composition Fe/(Fe+V)	Composition S/(Fe+V)	Method	Temp °C	Time h	Product
0.200	1.600	s. t[a)]	600	72	$(Fe, V)_5S_8$
	1.600	s. t	500	168	$(Fe, V)_5S_8+FeS_2$
0.500	1.160	s. t	700	336	$(Fe, V)_{1-\delta}S+(Fe, V)_3S_4$
	1.308	s. p. c[b)]	782	2	$(Fe, V)_{1-\delta}S+(Fe, V)_3S_4$
	1.315	s. p. c	727	5	$(Fe, V)_3S_4$
	1.366	s. p. c	622	5	$(Fe, V)_3S_4$
	1.380	s. t	570	168	$(Fe, V)_3S_4+FeS_2$
0.600	1.308	s. t	600	168	$(Fe, V)_{1-\delta}S+(Fe, V)_3S_4$
	1.317	s. t	570	168	$(Fe, V)_3S_4$
	1.357	s. t	570	168	$(Fe, V)_3S_4$
	1.377	s. t	570	408	$(Fe, V)_3S_4+FeS_2$
0.170	1.159	s. p. c	783	24	$(Fe, V)_{1-\delta}S$
	1.176	s. p. c	727	22	$(Fe, V)_{1-\delta}S+(Fe, V)_3S_4$
	1.310	s. t	570	21	$(Fe, V)_3S_4+(Fe, V)_{1-\delta}S$
	1.320	s. t	570	23	$(Fe, V)_3S_4+FeS_2$
	1.317	s. t	570	24	$(Fe, V)_3S_4$
0.800	1.250	s. t	570	82	$(Fe, V)_{1-\delta}S+(Fe, V)_3S_4$
	1.275	s. t	570	82	$(Fe, V)_{1-\delta}S+(Fe, V)_3S_4+FeS_2$
	1.300	s. t	570	83	$(Fe, V)_{1-\delta}S+(Fe, V)_3S_4+FeS_2$

a) Sealed tube method. b) Sulfur pressure control method.

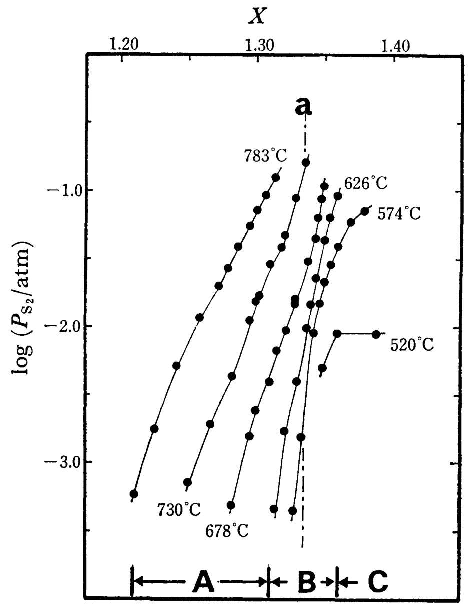

Fig. 2. P_{S_2}-composition isotherms of $Fe_{0.60}V_{0.40}S_X$. A: $(Fe,V)_{1-\delta}S$ s.s.+$(Fe,V)_3S_4$ s.s. B: $(Fe_{0.60}V_{0.40})_3S_4$ s.s. C: $(Fe,V)_3S_4$ s.s.+FeS_2. a: Stoichiometric Fe+V: S=3 : 4 composition.

Figure 1 shows isotherms with the composition $Fe_{0.50}V_{0.50}S_x$, where X ranges between 1.25 and 1.41 within the experimental temperature region. In this compositional range, several kinds of quenched specimens were identified by X-ray powder diffraction patterns. The following phases were found: hexagonal $(Fe,V)_{1-\delta}S$ s.s., monoclinic V_3S_4-type $(Fe,V)_3S_4$ s.s., and cubic FeS_2 (pyrite). In the range of composition between $X=1.25$ and $X=1.31$, a two-phase mixture of $(Fe,V)_{1-\delta}S$ s.s. and $(Fe,V)_3S_4$ s.s. was obtained below 814 °C. One phase of $(Fe_{0.50}V_{0.50})_3S_4$ s.s. was observed in the range $1.31 \leqq X \leqq 1.37$. Beyond $X=1.37$, FeS_2 appeared together with $(Fe,V)_3S_4$ s.s. at temperatures below 622 °C.

As shown in Fig.1, the steepest part of the isothermal curves is observed at the composition of about $X=1.33$, accompanied by the rapid change of sulfur pressure. This feature of the isotherms in the one-phase region clearly indicates the existence of a stoichiometric (Fe+V):S=3 : 4 phase at temperatures below 727 °C. It is noted that isothermal curves for 814, 782, and 727 °C change their slopes slightly at about $X=1.31$. This composition corresponds to the metal-rich phase boundary of $(Fe_{0.50}V_{0.50})_3S_4$ s.s., which was determined from X-ray measurements of quenched specimens. In a two-phase field ($1.25<X<1.31$), however, the isotherms are not horizontal, as is often observed in the case of a two-phase equilibrium of binary systems, but represent rather a continuous variation of sulfur pressure with composition. The sulfur-rich limit of the $(Fe_{0.50}V_{0.50})_3S_4$ phase extends to the composition of $X=1.37$, where the isotherm becomes horizontal at 521°C due to the formation of FeS_2. However, the curvature change of the isotherm for 572 °C is observed at $X=1.38$ rather than at $X=1.37$. This suggests that the homogeneity range of $(Fe_{0.50}V_{0.50})_3S_4$ phase tends to be broadened slightly to the sulfur-rich side with increasing temperature.

A few remarks should be made here regarding the powder X-ray diffraction patterns of the FeS_2, which coexist with $(Fe,V)_3S_4$ s.s. phase. All the unit cell dimensions of FeS_2 in equilibrium with $(Fe,V)_3S_4$ s.s. are the same as those of pure FeS_2, within the limits of error. It may be concluded that FeS_2 does not take measurable amounts of vanadium or sulfur into solid solution and is a stoichiometric compound.

Figure 2 shows isotherms with the composition $Fe_{0.60}$-

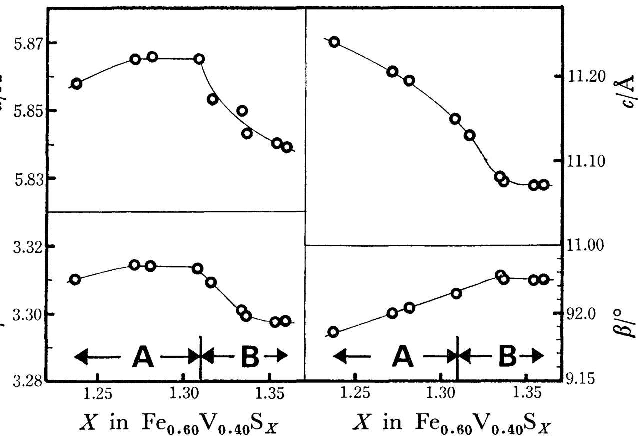

Fig. 3. Relationship between lattice constants of the coexisting phase ($(Fe,V)_3S_4$ s.s.) and the bulk composition. Region, A, is a two-phase field and region, B, a one-phase field.

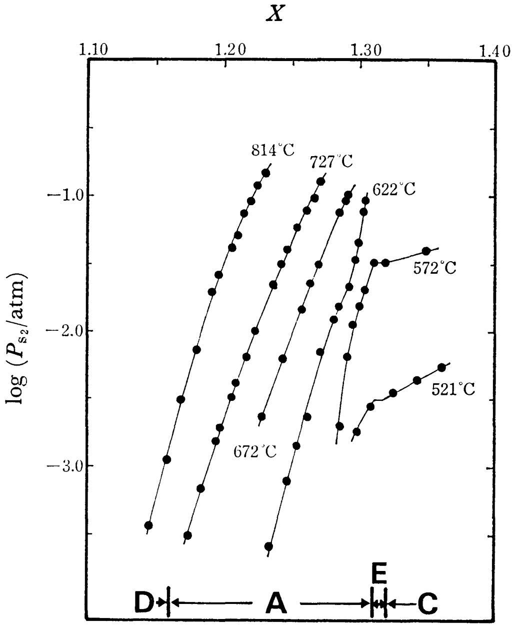

Fig. 4. P_{S_2}-composition isotherms of $Fe_{0.71}V_{0.29}S_X$. A: $(Fe,V)_{1-\delta}S$ s.s.+$(Fe,V)_3S_4$ s.s. C: $(Fe,V)_3S_4$ s.s.+FeS_2. D: $(Fe_{0.71}V_{0.29})_{1-\delta}S$ s.s. E: $(Fe,V)_{1-\delta}S$+$(Fe,V)_3S_4$ s.s.+FeS_2.

$V_{0.40}S_X$, where X ranges between 1.21 and 1.39. As listed in Table 1, the following phase relations are found: a two-phase mixture of $(Fe,V)_{1-\delta}S$ s.s. and $(Fe,V)_3S_4$ s.s., $(Fe_{0.60}V_{0.40})_3S_4$ s.s. phase, and a two-phase mixture of FeS_2 and $(Fe,V)_3S_4$ s.s. in the compositional range of $X<1.31$, $1.31\leqq X\leqq 1.36$, and $1.36<X$, respectively.

Although the metal-rich phase boundary of $(Fe_{0.60}V_{0.40})_3S_4$ is determined to be about $X=1.31$ by X-ray powder diffraction of quenched specimens, no characteristic change of the curvature is observed at $X=1.31$ in the isotherms for 783, 730, and 678 °C. These isotherms exhibit rather continuous and gradual changes of sulfur pressure with composition. Within the one-phase region, a rapid increase of pressure is observed near the stoichiometric composition ($X=1.33$) at temperatures below 678 °C. This indicates the existence of the stoichiometric $(Fe_{0.60}V_{0.40})_3S_4$ phase. The isotherm for 520 °C is clearly horizontal at the composition of about $X=1.36$, due to the formation of FeS_2 in equilibrium with $(Fe,V)_3S_4$ solid solution. However, the isotherm for 574 °C does not show such an abrupt change of the slope as is observed at 520 °C.

In order to clarify the behavior of the isotherms on the metal-richer side beyond $X=1.31$, lattice parameters of several specimens quenched from 730 °C were examined by X-ray diffraction (Cu $K\alpha$). Figure 3 shows the relationships between the lattice constant of the coexisting phase ($(Fe,V)_3S_4$ s.s.) and the bulk composition within a two-phase field ($X<1.31$). The lattice constant c and β-angle of $(Fe,V)_3S_4$ s.s. in equilibrium with $(Fe,V)_{1-\delta}S$ s.s. change continuously with compositions, the lattice constants a and b remaining nearly the same in the range $1.27<X<1.31$. In general, shifts of lattice constant correspond to the compositional variation of the phase. Therefore, it may be concluded that solid solution limits of $(Fe,V)_3S_4$ phase vary smoothly with the equilibrium sulfur pressure, which is represented as the isothermal curve for 730 °C in Fig.2.

The high-temperature X-ray diffraction studies were made on a two-phase mixture of $(Fe,V)_3S_4$ s.s. and $(Fe,V)_{1-\delta}S$ s.s. with bulk composition of $X=1.28$ in order to observe the real phase relations directly. It was confirmed that (1) a high-temperature phase with trigonal structure is formed at temperatures above 850 °C due to the reaction of $(Fe,V)_{1-\delta}S$ s.s. with $(Fe,V)_3S_4$ s.s. and (2) the phase is unquenchable and readily inverts to the original, two different phases on quenching below 850 °C. From these results, the behavior of the isotherms for 783 and 730 °C may be interpreted as reflecting the sulfur activity change of solids at the intermediate state of phase formation or separation.

Figure 4 shows isotherms with the composition $Fe_{0.71}V_{0.29}S_X$, richer in Fe than that in Fig. 2. The region covered experimentally lies in the compositional range of $1.15<X<1.37$. From X-ray studies of the quenched specimens, the following phase relations were confirmed: $(Fe_{0.71}V_{0.29})_{1-\delta}S$ phase, a two-phase mixture of $(Fe,V)_{1-\delta}S$ s.s. and $(Fe,V)_3S_4$ s.s., and a two-phase mixture of $(Fe,V)_3S_4$ s.s. and FeS_2, in the compositional ranges of $X\leqq 1.16$, $1.16<X<1.315$, and $1.32\leqq X$, respectively.

With regard to the isotherm feature, it is noted that the isotherm for 814°C does not show any characteristic change of the curvature at the sulfur-rich limits of $(Fe_{0.71}V_{0.29})_{1-\delta}S$ phase ($X=1.16$) and exhibits continuous variations of sulfur pressure with composition in the range of $1.15<X<1.23$. This seemed to be indicative of the existence of a high-temperature phase. In this connection, X-ray studies of specimens with the bulk composition of $X=1.20$ were carried out at high temperatures. It was found that a two-phase mixture of $(Fe,V)_{1-\delta}S$ s.s. and $(Fe,V)_3S_4$ s.s. transforms to the high-temperature hexagonal $(Fe_{0.71}V_{0.29})_{0.83}S$ phase perfectly at temperatures above 800 °C. Therefore, it may be suggested that the homogeneity range of the high-temperature phase extends to $X=1.23$ under the present experimental conditions and, when quenching, the specimens whose composition is richer than $X=1.16$ decompose to $(Fe,V)_{1-\delta}S$ and $(Fe,V)_3S_4$ s.s. phases.

The slope of isotherms for 572 and 521 °C changes abruptly at the composition of $X=1.31$ and a relatively small change in the pressure causes a large variation of the composition. The behavior of these isotherms may be interpreted in the same way as in the case of isotherms of $Fe_{0.60}V_{0.40}S_X$ for 520 °C. That is to say, FeS_2 begins to be formed at the composition above $X=1.31$ and the isotherms become horizontal.

However, the X-ray powder diffraction pattern of the specimen with the composition of $X=1.317$ seemed to show only the presence of one phase, $(Fe,V)_3S_4$ (Table 1); this result is inconsistent with the observation in Fig. 3. This is considered to originate from the difficulty that the small amount of $(Fe,V)_{1-\delta}S$ and FeS_2 in equilibrium with $(Fe, V)_3S_4$ can hardly be detected by X-ray powder analysis. On the basis of *in situ* observations described above, it can therefore be presumed that the three-phase field containing $(Fe, V)_{1-\delta}S$, $(Fe, V)_3S_4$, and FeS_2 occurs in the range $1.31<X<1.32$.

Tentative Phase Diagram of the Fe–V–S System at 570 °C. The isothermal tentative phase diagram in a part of the Fe–V–S system at about 570 °C was constructed mainly on the basis of the results of thermogravimetry. The phase relations and their compositional limits are summarized in Fig. 5.

Phase relations in parts of the Fe–S system at elevated temperatures have been clarified by earlier workers. Kullerud and Yoder²⁾ found that FeS_2 (pyrite), which has a cubic structure (Pa3), shows very little departure from the stoichiometric composition and melts incongruently at 743 °C. Arnold⁴⁾ studied equilibrium relations between $Fe_{1-\delta}S$ (pyrrhotite) and FeS_2 (pyrite) from 325 to 743 °C and determined the $Fe_{1-\delta}S$ solvus curve which represents the sulfur-rich limit of $Fe_{1-\delta}S$ coexisting with FeS_2. It is inferred from these studies that only two phases, $Fe_{1-\delta}S$ and FeS_2, are stable at about 570 °C. The sulfur-rich limit of $Fe_{1-\delta}S$ reaches about 46.2 atom%Fe at 570 °C, as can be estimated from Arnold's data.

The V–S system has recently been studied by many investigators. However, some inconsistencies exist in the reports, with respect to the phase relations and the homogeneity range of the phase. Using X-ray powder diffraction patterns of quenched specimens, de Vries and Jellinek³⁾ studied the V–S system, and reported that orthorhombic VS (range VS—$VS_{1.06}$), hexagonal $V_{1-\delta}S$ (range $VS_{1.06}$—$VS_{1.18}$), monoclinic V_3S_4 (range $VS_{1.20}$—$VS_{1.52}$), monoclinic V_5S_8 ($VS_{1.56}$), and trigonal V_3S_5 exist in the range VS—$VS_{1.67}$ at room temperature. Also, they found that the orthorhombic MnP-type VS transforms into hexagonal NiAs-type at about 600 °C for VS and at 350 °C for $VS_{1.05}$. Nakahira *et al.*⁵⁾ investigated the phase relations of the V–S system at 727 °C through *in situ* observations by means of a quartz spring balance and suggested the existence of sesquisulfide V_2S_3 with the homogeneity range of $VS_{1.45}$—$VS_{1.54}$. Recently, Wakihara *et al.*⁶⁾ examined the equilibrium phase relation between V_3S_4 and V_5S_8 in detail at temperatures from 650 to 800 °C and found that V_2S_3 appears to form below about 750 °C due to the phase separation of high-temperature V_3S_4, and that the homogeneity range of V_2S_3 extends from $VS_{1.446}$ to $VS_{1.520}$ at 650 °C. However, the existence of a V_2S_3 phase has not been confirmed at all from crystallographic viewpoint, because the X-ray diffraction pattern of the quenched V_2S_3 phase was very similar to that of the V_3S_4 phase. From the study of the chemical transport in the V–S system, Saeki *et al.*⁷⁾ found that the homogeneity range of V_5S_8 phase extends from $VS_{1.57}$ to about $VS_{1.64}$. The author showed in the previous paper¹⁾ that the two-phase field of $(Fe,V)_2S_3$–$(Fe,V)_5S_8$ exists in the range from $X=1.55$ to $X=1.56$ at 622 °C, on the basis of experimental results of a part of the Fe–V–S system at sections with atomic Fe:V ratio 1 : 19.

A survey of the literature on the V–S system indicates that further detailed comprehensive studies are desirable to draw accurate phase diagrams at several temperatures. In the present study, the following phase relations of the V–S system are assumed for convenience: hexagonal $V_{1-\delta}S$ (range VS—$VS_{1.18}$), monoclinic V_3S_4 (range $VS_{1.20}$—$VS_{1.45}$), monoclinic V_2S_3 (range $VS_{1.46}$—$VS_{1.55}$), and monoclinic V_5S_8 (range $VS_{1.56}$—$VS_{1.64}$) exist at 570 °C. The trigonal V_3S_5 phase is omitted in this paper due to lack of data on its phase relation, homogeneity range, and equilibrium sulfur pressure and the possibility that it belongs to a high-pressure phase, as suggested by Nakano-Onoda *et al.*⁸⁾

The sulfur-rich and poor limits of $(Fe,V)_3S_4$ phase are determined by a smooth fitting of the data points which are obtained in this study. The sulfur-rich boundary recedes progressively toward sulfur-poor compositions with increasing Fe content; the upper sulfur solubility limits are 58.0 and 57.8 atom % S in sections with atomic Fe : V ratio 1 : 1 and 3 : 2, respectively. On the contrary, the sulfur-poor limit of $(Fe,V)_3S_4$ phase shows a constant value of 56.7 atom % S in spite of a variation in Fe : V ratio like that described above. This boundary is drawn in Fig. 5 as a straight line in parallel with that joining VS–FeS. The Fe-rich limit of $(Fe,V)_3S_4$ s.s. phase reaches to about $0.30=V/(Fe+V)$ ratio.

Solubility of Fe in the V_5S_8 phase was determined by the supplemental, quench-type, rigid tube experiment (Table 1). The Fe-rich limit of $(Fe,V)_5S_8$ phase was confirmed to reach about 0.20, $Fe/(Fe+V)$ ratio, at 600 °C. This value is in good agreement with the Fe-rich limit of the $(Fe,V)_5S_8$ phase, which was reported by Oka *et al.*⁹⁾ As shown in Fig. 5, the phase boundary of $(Fe,V)_3S_4$, $(Fe,V)_2S_3$, and $(Fe, V)_5S_8$ on the side richer in V than $V/Fe=1$ is determined by a smooth fitting of data points. Two-phase regions of $(Fe,V)_3S_4$–$(Fe,V)_2S_3$ and $(Fe,V)_2S_3$–$(Fe,V)_5S_8$ are extended in parallel with the line joining FeS–VS from the VS–S side to the Fe-rich phase boundaries.

With respect to the lower part of the FeS–VS–S diagram, it is assumed that $Fe_{1-\delta}S$ and $V_{1-\delta}S$ phases form a complete $(Fe,V)_{1-\delta}S$ solid solution at 570 °C. With homogeneous ranges of compounds, as previ-

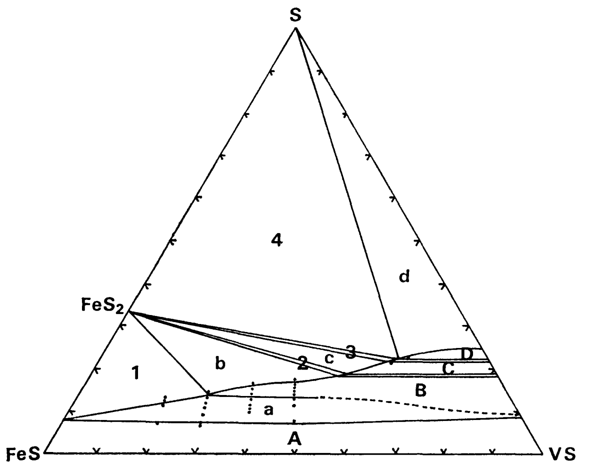

Fig. 5. Tentative phase diagram of the sulfur-rich portion of the Fe–V–S system at about 570 °C. Phase relations are represented as follows. Phase A: Monosulfide s.s. $(Fe,V)_{1-\delta}S$. B: $(Fe,V)_3S_4$ s.s. C: $(Fe,V)_2S_3$ s.s. D: $(Fe,V)_5S_8$ s.s. Two-phase regions are a: $(Fe,V)_3S_4$ s.s.+$(Fe,V)_{1-\delta}S$ s.s. b: $(Fe,V)_3S_4$ s.s.+FeS_2. c: $(Fe,V)_2S_3$ s.s.+FeS_2. d: $(Fe,V)_5S_8$ s.s.+L. Numbers in figure mean the univariant assemblages as follows. 1: FeS_2+$Fe_{1-\delta}S$+$(Fe,V)_3S_4$ s.s.+v. 2: FeS_2+$(Fe,V)_3S_4$ s.s.+$(Fe,V)_2S_3$ s.s.+v. 3: FeS_2+$(Fe,V)_2S_3$ s.s.+$(Fe,V)_5S_8$ s.s.+v. 4: FeS_2+$(Fe,V)_5S_8$ s.s.+L+v.

ously determined by Toulmin and Barton[10] and Arnold[4] for $Fe_{1-\delta}S$, and de Vries and Jellinek[3] for $V_{1-\delta}S$, it was possible to draw a monosulfide solid solution field of $(Fe,V)_{1-\delta}S$. This boundary is drawn qualitatively by a full line. The sulfur-rich limit of the monosulfide s.s. field reaches a maximum of 54.1 atom %S in the V–S side. It recedes progressively toward S-poor compositions with increasing Fe content till it reaches the middle part of the field. However, the upper sulfur solubility limits of monosulfide s.s. field are largely interpretative because of the lack of experimental data for compositions of $(Fe,V)_{1-\delta}S$ coexisting with $(Fe,V)_3S_4$.

As shown in Fig. 5, there are four univariant assemblages: $Fe_{1-\delta}S$–FeS_2–$(Fe,V)_3S_4$ s.s.-v, FeS_2–$(Fe,V)_3S_4$ s.s.–$(Fe,V)_2S_3$ s.s.–v, $(Fe,V)_2S_3$ s.s.–$(Fe,V)_5S_8$ s.s.–FeS_2-v, and FeS_2–$(Fe,V)_5S_8$ s.s.–L-v.

Relation of Lattice Parameters of $(Fe,V)_3S_4$ s.s. Phase with Composition. The $(Fe,V)_3S_4$ s.s. phase has the monoclinic V_3S_4-type structure (nonreduced space group I2/m referred to the fundamental NiAs-type cell), in which metal vacancies are ordered within alternate metal layers.[11] In the course of continuing the equilibrium study of the Fe–V–S system, several kinds of quenched specimens in the $(Fe,V)_3S_4$ s.s. field were examined by the X-ray powder diffraction technique in order to clarify the relation of lattice constant and composition. The lattice constants were calculated by the least-squares method from the data of powder diffractometer measurements using Cu $K\alpha$ radiation. Values of at least 20 reflections in the 2θ range of 10° to 70° were used in this computation. The compositional dependence of the unit cell dimensions are shown in Fig. 6—8.

It is found that the axial dimensions of the a-, b-, and c-axes and thus the cell volume decrease with increasing S content under the present experimental conditions. Also, the axial dimensions of the c-axis and the unit cell volume of $(Fe,V)_3S_4$ s.s. phase decrease with increasing Fe/V ratio, when the S/(Fe+V) ratio is held constant. This is in good agreement with that of $(Fe_xV_{1-x})V_2S_4$, which has been reported by Oka *et al.*[9] The c-dimensions of $(Fe,V)_3S_4$ with Fe:V=3 : 2 atomic ratio are about 2.6% smaller than that of V_3S_4.

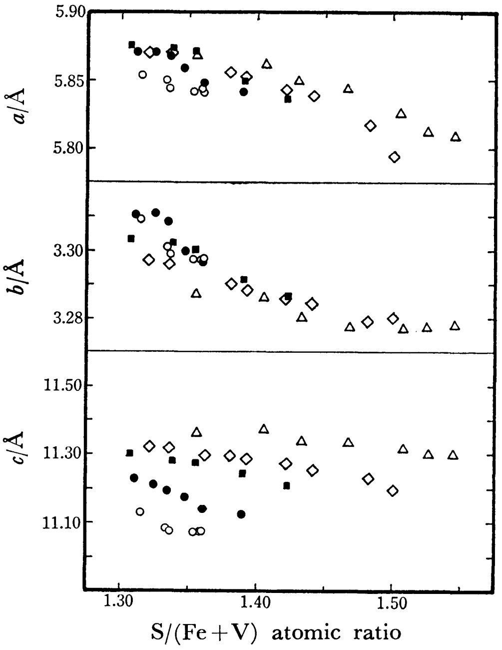

Fig. 6. Lattice constants of the unit cell of $(Fe,V)_3S_4$ s.s. phase as function of composition. △: Fe:V=1:19, ◇: Fe:V=13:37, ■: Fe:V=7:13, ●: Fe:V=1:1, ○: Fe:V=3:2.

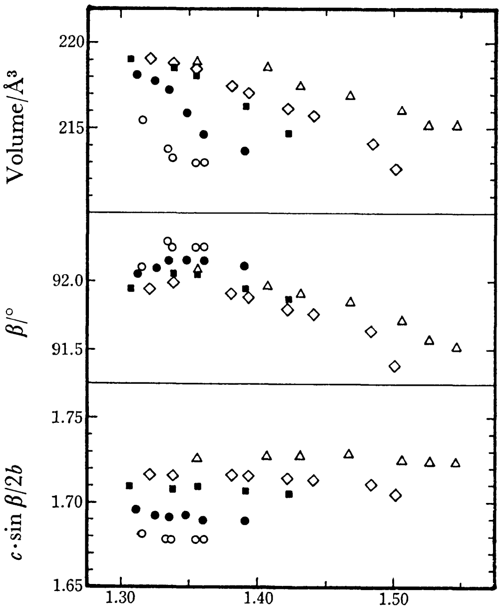

Fig. 7. Volume, β-angle and $c\cdot\sin\beta/2b$ of the unit cell of $(Fe,V)_3S_4$ s.s. phase as function of composition.

As shown in Fig. 7, however, the behavior of the β-angle of the unit cell is quite different from those

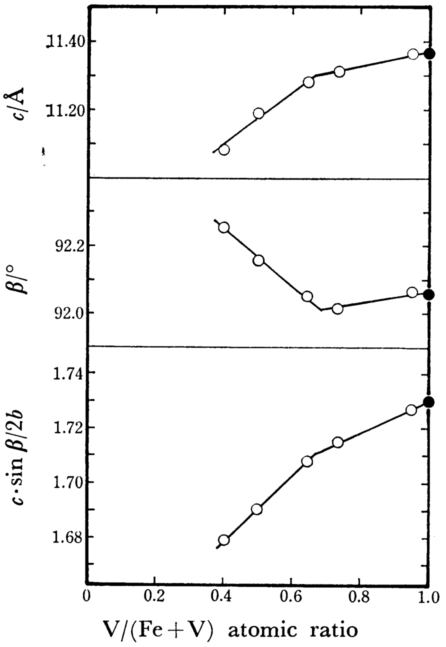

Fig. 8. Relation of c-dimension, β-angle and c·sinβ/2b of $(Fe,V)_3S_4$ compound with V/(Fe+V) atomic ratios. ●: De Vries and F. Jellinek (1974). ○: Present work.

of the a-, c-dimensions and the unit cell volume. Maximum values are observed at about $X=1.34$—1.35 in β-angle-composition relations of compounds with a constant Fe:V ratio. Also, the β-angle varies with the degree of the substitution of Fe for V in V_3S_4. It is apparent from Figs. 7 and 8 that the β-angle decreases with increasing Fe content in the range of V/(Fe+V), from 1 to about 0.70, and increases with increasing Fe content in the range of V/(Fe+V), from 0.7 to 0.4.

In order to examine the directional character of the structure for several $(Fe,V)_3S_4$ s.s. phases, the c·sin β/2b ratio in the monoclinic V_3S_4-type structure is calculated instead of the axial ratio of c/a in NiAs-type structure. As is evident in Fig. 7, the values of c·sin β/2b of compounds with the constant Fe/V ratio are nearly equal over the whole range of composition. On the other hand, when the S content is held constant, the ratio value decreases with increasing Fe content. This result indicates that the interlayer spacing is reduced relative to the intralayer spacing by the substitution of Fe for V in V_3S_4.

Figure 8 shows the relations of c-dimension, β-angle, and c·sin β/2b with V/(Fe+V) atomic ratio at the composition of about $X=1.33$. Data points do not fall on the same straight line and a change of the slope is observed at about V/(Fe+V)=0.67, whose composition corresponds to FeV_2S_4. From this results, it seems that the $(Fe,V)_3S_4$ s.s. phase can be divided into two types: one is the V_3S_4–FeV_2S_4 series, and the other is the FeV_2S_4–Fe_2VS_4 series. From the neutron diffraction studies of FeV_2S_4 compound,[12] it was found that all Fe atoms are confined to the partially filled metal layers and all V atoms to the filled metal layers. However, whether the $(Fe,V)_3S_4$ compound richer in Fe than FeV_2S_4 is an ordered phase or not as for the distribution of Fe and V atoms over all the metal sites is still an open question. Further detailed studies on the crystal structure and physical properties of $(Fe,V)_3S_4$ s.s. phase are necessary for a better understanding of the phase relations of the Fe–V–S system.

The author wishes to express his deep gratitude to professor Mitsuoki Nakahira of Okayama College of Science for his encouragement and helpful discussion throughout this study. Thanks are also due to Dr. H. Nakazawa for his guidance of the high-temperature X-ray measurements.

References

1) H. Wada, *Bull. Chem. Soc. Jpn.*, **51**, 1368 (1978).
2) G. Kullerud and H. S. Yoder, *Econ. Geol.*, **54**, 533 (1959).
3) A. B. De Vries and F. Jellinek, *Rev. Chim. Miner.*, **11**, 624 (1974).
4) R. G. Arnold, *Econ. Geol.*, **75**, 72 (1962).
5) M. Nakahira, K. Hayashi, M. Nakano-Onoda, and K. Shibata, "Proc. 8th Int. Symp. on the Reactivity of Solids," ed by J. Wood *et al.*, Plenum Press, New York (1977), pp. 397—401.
6) M. Wakihara, T. Uchida, and M. Taniguchi, *Metall. Trans.*, **9B**, 29 (1978).
7) M. Saeki, M. Nakano, and M. Nakahira, *J. Crystal Growth*, **24/25**, 154 (1974).
8) M. Nakano-Onoda, S. Yamaoka, K. Yukino, K. Kato, and I. Kawada, *J. Less-Common Metals*, **44**, 341 (1976).
9) Y. Oka, K. Kosuge, and S. Kachi, *Mat. Res. Bull.*, **12**, 1117 (1977).
10) P. Toulmin, III, and P. B. Barton, Jr., *Geochim. Cosmochim. Acta*, **28**, 641 (1964).
11) M. Cheverton and A. Sapet, *C. R. Acad. Sci., Paris*, **261**, 928 (1965).
12) I. Kawada, N. Niimura, M. Isobe, and H. Wada, *Res. Rep. Lab. Nucl. Sci. Tohoku Univ.*, **11**, 226 (1978).